KMT2D mutations and *TP53* disruptions are poor prognostic biomarkers in mantle cell lymphoma receiving high-dose therapy: a FIL study

Simone Ferrero,[1,2*] Davide Rossi,[3,4*] Andrea Rinaldi,[4*] Alessio Bruscaggin,[4] Valeria Spina,[4] Christian W. Eskelund,[5,6] Andrea Evangelista,[7] Riccardo Moia,[8] Ivo Kwee,[4,9,10] Christina Dahl,[11] Alice Di Rocco,[12] Vittorio Stefoni,[13] Fary Diop,[8] Chiara Favini,[8] Paola Ghione,[1] Abdurraouf Mokhtar Mahmoud,[8] Mattia Schipani,[8] Arne Kolstad,[14] Daniela Barbero,[1] Domenico Novero,[15] Marco Paulli,[16] Alberto Zamò,[17,18] Mats Jerkeman,[19] Maria Gomes da Silva,[20] Armando Santoro,[21] Annalia Molinari,[22] Andres Ferreri,[23] Kirsten Grønbæk,[5,6] Andrea Piccin,[24] Sergio Cortelazzo,[25] Francesco Bertoni,[4#] Marco Ladetto[26#] and Gianluca Gaidano[8#]

[1]Department of Molecular Biotechnologies and Health Sciences - Hematology Division, Università di Torino, Torino, Italy; [2]Hematology Division, AOU Città della Salute e della Scienza di Torino, Torino, Italy; [3]Hematology, Oncology Institute of Southern Switzerland, Bellinzona, Switzerland; [4]Universita' della Svizzera italiana, Institute of Oncology Research, Bellinzona, Switzerland; [5]Department of Hematology, Rigshospitalet, Copenhagen, Denmark; [6]Biotech Research and Innovation Centre, Copenhagen, Denmark; [7]Clinical Epidemiology, Città della Salute e della Scienza and CPO Piemonte, Torino, Italy; [8]Division of Hematology, Department of Translational Medicine, University of Eastern Piedmont, Novara, Italy; [9]Swiss Institute of Bioinformatics (SIB), Lausanne, Switzerland; [10]Dalle Molle Institute for Artificial Intelligence (IDSIA), Manno, Switzerland; [11]Danish Cancer Society Research Center, Copenhagen, Denmark; [12]Department of Cellular Biotechnologies and Hematology, Policlinico Umberto I, "Sapienza" University of Rome, Roma, Italy; [13]Institute of Hematology "L. e A. Seràgnoli", University of Bologna, Bologna, Italy; [14]Department of Oncology, Oslo University Hospital, Oslo, Norway; [15]First Unit of Pathology, AOU Città della Salute e della Scienza di Torino, Torino, Italy; [16]Unit of Anatomic Pathology, Department of Molecular Medicine, Fondazione IRCCS Policlinico San Matteo and Università degli Studi di Pavia, Pavia, Italy; [17]Department of Oncology, Università di Torino, Torino, Italy; [18]Department of Diagnostics and Public Health, University of Verona, Verona, Italy; [19]Department of Oncology, Lund University Hospital, Lund, Sweden; [20]Department of Hematology, Instituto Português de Oncologia de Lisboa, Lisboa, Portugal; [21]Humanitas Cancer Center, Humanitas Clinical and Research Center, Rozzano, Italy; [22]Hematology, Ospedale degli Infermi, Rimini, Italy; [23]Lymphoma Unit, Department of Onco-Haematology, IRCCS San Raffaele Scientific Institute, Milano, Italy; [24]Department of Hematology, Ospedale Generale, Bolzano, Italy; [25]Oncology Unit, Humanitas/Gavazzeni Clinic, Bergamo, Italy and [26]SC Ematologia, Azienda Ospedaliera Santi Antonio e Biagio e Cesare Arrigo, Alessandria, Italy

**SF, DR and AR contributed equally as co-first authors.*

#FB, ML and GG contributed equally as co-senior authors.

 doi:10.3324/haematol.2018.214056

Received: December 24, 2018.

Accepted: September 19, 2019.

Pre-published: September 19, 2019.

Correspondence: *SIMONE FERRERO* - simone.ferrero@unito.it

SUPPLEMENTARY APPENDIX

KMT2D mutations and *TP53* disruptions are poor prognostic biomarkers in MCL receiving high-dose therapy: a FIL study

Simone Ferrero[1,2], Davide Rossi*[3,4], Andrea Rinaldi*[4], Alessio Bruscaggin[4], Valeria Spina[4], Christian W Eskelund[5,6], Andrea Evangelista[7], Riccardo Moia[8], Ivo Kwee[4,9,10], Christina Dahl[11], Alice Di Rocco[12], Vittorio Stefoni[13], Fary Diop[8], Chiara Favini[8], Paola Ghione[1], Abdurraouf Mokhtar Mahmoud[8], Mattia Schipani[8], Arne Kolstad[14], Daniela Barbero[1], Domenico Novero[15], Marco Paulli[16], Alberto Zamò[17,18], Mats Jerkeman[19], Maria Gomes da Silva[20], Armando Santoro[21], Annalia Molinari[22], Andres Ferreri[23], Kirsten Grønbæk[5,6], Andrea Piccin[24], Sergio Cortelazzo[25], Francesco Bertoni°[4], Marco Ladetto°[26] and Gianluca Gaidano°[8]*

[1]Department of Molecular Biotechnologies and Health Sciences - Hematology Division, Università di Torino, Torino, Italy; [2]Hematology Division, AOU Città della Salute e della Scienza di Torino, Torino, Italy; [3]Hematology, Oncology Institute of Southern Switzerland, Bellinzona, Switzerland; [4]Universita' della Svizzera italiana, Institute of Oncology Research, Bellinzona, Switzerland; [5]Department of Hematology, Rigshospitalet, Copenhagen, Denmark; [6]Biotech Research and Innovation Centre, Copenhagen, Denmark; [7]Clinical Epidemiology, Città della Salute e della Scienza and CPO Piemonte, Torino, Italy; [8]Division of Hematology, Department of Translational Medicine, University of Eastern Piedmont, Novara, Italy; [9]Swiss Institute of Bioinformatics (SIB), Lausanne, Switzerland; [10]Dalle Molle Institute for Artificial Intelligence (IDSIA), Manno, Switzerland; [11]Danish Cancer Society Research Center, Copenhagen, Denmark; [12]Department of Cellular Biotechnologies and Hematology, Policlinico Umberto I, "Sapienza" University of Rome, Roma, Italy; [13]Institute of Hematology "L. e A. Seràgnoli", University of Bologna, Bologna, Italy; [14]Department of Oncology, Oslo University Hospital, Oslo, Norway; [15]First unit of Pathology, AOU

Città della Salute e della Scienza di Torino, Torino, Italy; [16]Unit of Anatomic Pathology, Department of Molecular Medicine, Fondazione IRCCS Policlinico San Matteo and Università degli Studi di Pavia, Pavia, Italy; [17]Department of Oncology, Università di Torino, Torino, Italy; [18]Department of Diagnostics and Public Health, University of Verona, Italy; [19]Department of Oncology, Lund University Hospital, Lund, Sweden; [20]Department of Hematology, Instituto Português de Oncologia de Lisboa, Lisboa, Portugal; [21]Humanitas Cancer Center, Humanitas Clinical and Research Center, Rozzano, Italy; [22]Hematology, Ospedale degli Infermi, Rimini, Italy; [23]Lymphoma Unit, Department of Onco-Haematology, IRCCS San Raffaele Scientific Institute, Milano, Italy; [24]Department of Hematology, Ospedale Generale, Bolzano, Italy; [25]Oncology Unit, Humanitas/Gavazzeni Clinic, Bergamo, Italy; [26]SC Ematologia, Azienda Ospedaliera Santi Antonio e Biagio e Cesare Arrigo, Alessandria, Italy.

* These Authors equally contributed as First Authors

° These Authors equally contributed as Senior Authors

SUPPLEMENTARY METHODS

Patients series

The FIL-MCL0208 (NCT02354313) is a phase III, multicenter, open-label, randomized, controlled study, designed to determine the efficacy of lenalidomide as maintenance versus observation in young (18-65 years old), fit, advanced stage (Ann arbor II-IV) MCL patients who achieved complete or partial remission after first line intensified and high-dose chemotherapy plus rituximab followed by ASCT. Briefly, patients received 3 R-CHOP-21, followed by R-high-dose cyclophosphamide (4g/m2), 2 cycles of R-high-dose Ara-C (2g/m2 q12x3 d) and ASCT conditioned by using the BEAM or FEAM regimen. From May 2010 to August 2015, a total of 300 patients were enrolled in the study. Cases of non-nodal MCL were excluded.[1] All patients required to have a biopsy proving MCL, including evidence of cyclin D1 overexpression or t(11;14)(q13;q32) translocation. MCL diagnosis was confirmed by centralized pathological revision according to WHO criteria.[1] The clinical trial, as well as the ancillary mutational study, were approved by the Ethical Committees of all the enrolling Centers. All patients provided written informed consent for the use of their biological samples for research purposes, in accordance with Institutional Review Boards requirements and the Helsinki's declaration. Clinical results of the fist interim analysis of the trial were already presented.[2] Final, unblinded results are not available at the moment and have not been yet presented anywhere.

Biological samples

Bone marrow (BM) and peripheral blood (PB) samples were collected, as per protocol, at baseline and at several time-points during follow-up, corresponding to the pre-planned time-points for minimal residual disease (MRD) analysis. To identify and quantify the rate of tumor invasion, flow cytometry (FC) was performed both on BM and PB with the following antibodies: anti-CD19 APC, anti-CD23 PE, anti-CD5 FITC, and anti-CD20. Tumor cells were sorted from the baseline BM

samples by immunomagnetic beads (CD19 MicroBeads,human-Miltenyi Biotec GmbH, Bergisch Gladbach, Germany) and stocked as dry pellets.

Tumor DNA was extracted according to DNAzol protocol (Life Technologies). Germline DNA was obtained from PB mononuclear cells collected under treatment and proven to be tumor free by MRD analysis.

Next generation sequencing

A targeted resequencing panel (target region: 37'821 bp) (Table S1) including the coding exons and splice sites of 7 genes (*ATM, TP53, CCND1, WHSC1, KMT2D, NOTCH1* exon *34, BIRC3*) that are recurrently mutated in ≥ 5% of MCL tumors was specifically designed.[3-5] We also included in the panel *TRAF2* [6] and *CXCR4.*[7] The gene panel was analyzed in tumor DNA from baseline BM $CD19^+$ purified MCL cells (186 cases) and, for comparative purposes to filter out polymorphisms, in the paired normal genomic DNA (105 cases). NGS libraries preparation was performed using TruSeq Custom Amplicon sequencing assay according to manufacturer's protocol (Illumina, Inc., San Diego, CA). Multiplexed libraries (n=48 per run) were sequenced using 300-bp paired-end runs on an Illumina MiSeq sequencer, (median depth of coverage 2356x). To avoid the loss of *NOTCH1* ex 34 c.7544_7545delCT mutation, that is included in a region poorly covered by the target design, all MCL cases were also analyzed by amplification refractory mutation system (ARMS) polymerase chain reaction (PCR).

Bioinformatic analysis

FASTQ sequencing reads were locally aligned to the hg19 version of the human genome assembly using the BWA v.0.6.2 software with the default setting, and sorted, indexed and assembled into a mpileup file using SAMtools v.1. The aligned read families were processed with mpileup. A cut-off of 10% of variant allele frequency (VAF) was set for variant calling. Among cases provided with both tumor and paired normal gDNA, single nucleotide variations and indels were called using

the somatic function of VarScan2. The variants called by VarScan2 were annotated by using the SeattleSeq Annotation 138 tool by using the default setting. Variants annotated as SNPs according to dbSNP 138 (with the exception of *TP53* variants that were manually curated and scored as SNPs according to the IARC *TP53* database), intronic variants mapping >2 bp before the start or after the end of coding exons, and synonymous variants were then filtered out. The following strict post-processing filters were then applied to the remaining variants to further improve variant call confidence. Accordingly, variants represented in >10 reads of the paired germline and/or variants with a somatic p value from VarScan2 >$3.305e^{-7}$ [multiple comparisons corrected p threshold=$3.305e^{-7}$, corresponding to alpha of 0.05/(37'821 x 4 alleles per position)] were no further considered. Variant allele frequencies for the resulting candidate mutations and the background error rate were visualized using IGV. Among patients lacking the paired normal gDNA, single nucleotide variations and indels were called in tumor gDNA with the *cns* function of VarScan2. The variants called by VarScan2 were annotated by using the SeattleSeq Annotation 138 tool by using the default setting. Variants annotated as SNPs according to dbSNP 138 (with the exception of *TP53* variants that were manually curated and scored as SNPs according to the IARC *TP53* database), intronic variants mapping >2 bp before the start or after the end of coding exons, and synonymous variants were then filtered out. Only protein truncating variants (i.e. indels, stop codons and splice site mutations), as well as missense variants not included in the dbSNP 138 and annotated as somatic in the COSMIC v78 database, were retained.

Copy number variation analysis

DNA profiling was performed on DNA samples derived from baseline BM CD19+ purified tumor cells using the HumanOmni2.5 arrays (Illumina, San Diego, CA, USA). Copy number status of the genes included in the targeted resequencing panel (*KMT2D* and *TP53*) was assessed after genomic profiles segmentation with the Fast First-derivative Segmentation Algorithm, as previously described.[8,9]

Minimal residual disease analysis

For MRD purposes, MCL diagnostic BM and PB samples were investigated for IGH gene rearrangements and BCL1/IGH MTC by qualitative PCR. Briefly, IGH were screened using forward consensus primers annealing the IGH-V-regions and a reverse primer complementary to the JH region. BCL1/IGH MTC translocation was investigated by nested-PCR approach, as described.[10-12] After direct sequencing, FASTA files alignment was performed by IMGT/V-QUEST (http://imgt.org) and BlastN tool (NCBI, https://blast.ncbi.nlm.nih.gov/Blast.cgi), in order to define rearranged loci nomenclature, chromosomic breakpoints, and to assess patient specific nucleotide insertions (N insertions), then used to design allele specific oligonucleotides primers for nested-PCR MRD monitoring. Therefore, both BM and PB samples were analyzed for MRD at specific time points during and after treatment.

Statistical analysis

The primary outcome of the clinical study was progression-free survival (PFS). PFS was calculated from the date of enrolment into the clinical study to the date of disease progression (event), death from any causes (event), or last follow up (censoring).[13] Secondary outcomes included overall survival (OS), measured from the date of enrolment into the clinical study to the date of death from any causes (event), or last follow up (censoring). Time-to-event outcomes (PFS and OS) were estimated using the Kaplan-Meier method and compared between groups using the Log-rank test. The adjusted effects of mutations and exposure variables (MIPI-c and blastoid variant) on PFS and OS were estimated by Cox regression. To compare clinical baseline features between patients enrolled in the molecular study and patients not included in the analysis, we used Mann-Whitney test for continuous variables and Pearson's chi-squared test for categorical variables. A Cox model for PFS was estimated including MIPI-c and clinically impacting genetic alterations, and an additive score was computed according to the proportion between each predictor coefficient and the lowest one. The Cox model was internally validated using 1000 bootstrap samples and the C-statistic correct

for optimism was also provided. Patients were then grouped in classes of risk according to their total score using the nonparametric tree modelling technique of classification and regression tree (CART) analysis. Statistical analyses were performed using Stata 13.0 and R 3.4.1. The outcome data for the present analysis were updated as of December, 2017 the randomization arms being still blinded.

SUPPLEMENTARY FIGURE LEGENDS

Figure S1. Survival analysis for patients enrolled in the MCL0208 clinical trial included and not included in the present molecular study. Kaplan-Meier estimates of progression free survival (A) and overall survival (B) of patients with available DNA included in the present molecular study (in blue) and of patients without available DNA not included in the present molecular study (in yellow). The Log-rank statistics *p* values are indicated adjacent curves.

Figure S2. Disposition of identified gene mutations across the protein. Mutations identified in the studied cohort are plotted above the protein divided into the main domains**.** Missense mutations are plotted in green, stop codon mutations in red, splicing mutations in black, frameshift mutations in red, in-frame mutations in yellow.

Figure S3. Prognostic impact of *TP53* mutation and *TP53* deletion. Kaplan-Meier estimates of progression free survival (A) and overall survival (B) of *TP53* mutated patients, *TP53* deleted patients, *TP53* mutated and deleted patients, versus wild type patients. Cases with *TP53* mutation are represented by the yellow line, cases with *TP53* deletion are represented by the red line, cases with *TP53* mutation and deletion are represented by the black line, cases without *TP53* mutation and deletion are represented by the blue line. The Log-rank statistics *p* values are indicated adjacent curves.

Figure S4. Prognostic impact of *NOTCH1* mutation and *ATM* mutation. Kaplan-Meier estimates of (A) progression free survival and (B) overall survival of patients harboring *NOTCH1* mutation and Kaplan-Meier estimates of (C) progression free survival and (D) overall survival of patients harboring *ATM* mutation. Cases harboring *NOTCH1* or *ATM* mutation are represented by the yellow line. Wild

type cases are represented by the blue line. The Log-rank statistics *p* values are indicated adjacent curves.

Figure S5. Prognostic impact of *WHSC1* mutation and *CCND1* mutation. Kaplan-Meier estimates of (A) progression free survival and (B) overall survival of patients harboring *WHSC1* mutations and Kaplan-Meier estimates of (C) progression free survival and (D) overall survival of patients harboring *CCND1* mutation. Cases harboring *WHSC1* or *CCND1* mutation are represented by the yellow line. Wild type cases are represented by the blue line. The Log-rank statistics *p* values are indicated adjacent curves.

Figure S6. Prognostic impact of *BIRC3* mutation and *TRAF2* mutation. Kaplan-Meier estimates of (A) progression free survival and (B) overall survival of patients harboring *BIRC3* mutation and Kaplan-Meier estimates of (C) progression free survival and (D) overall survival of patients harboring *TRAF2* mutation. Cases harboring *BIRC3* or *TRAF2* mutation are represented by the yellow line. Wild type cases are represented by the blue line. The Log-rank statistics *p* values are indicated adjacent curves.

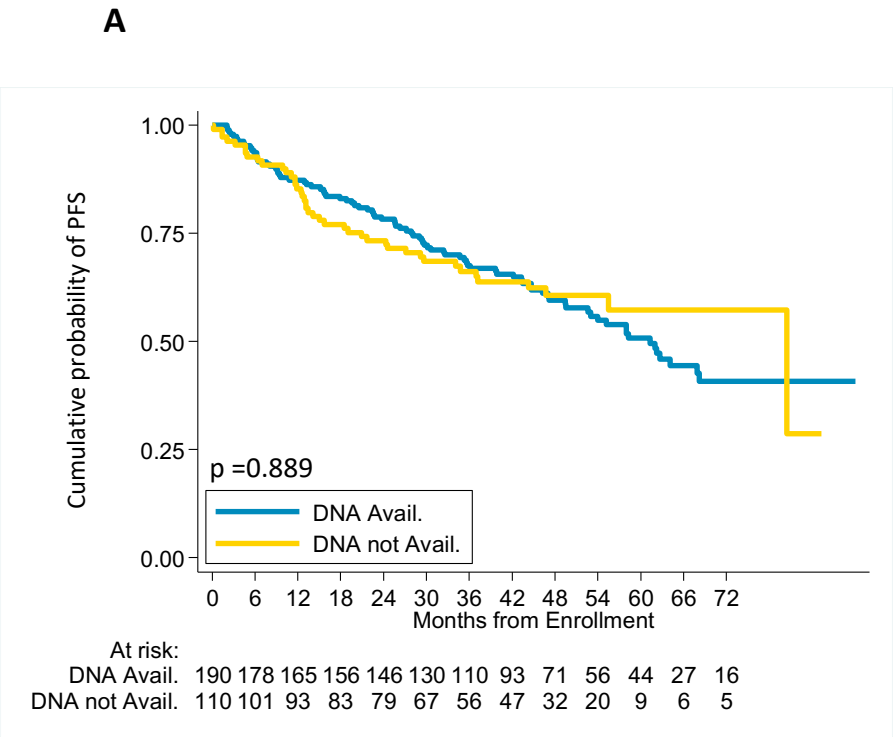
A
Cumulative probability of PFS
1.00
0.75
0.50
0.25
0.00
p =0.889
DNA Avail.
DNA not Avail.
0 6 12 18 24 30 36 42 48 54 60 66 72
Months from Enrollment
At risk:
DNA Avail. 190 178 165 156 146 130 110 93 71 56 44 27 16
DNA not Avail. 110 101 93 83 79 67 56 47 32 20 9 6 5

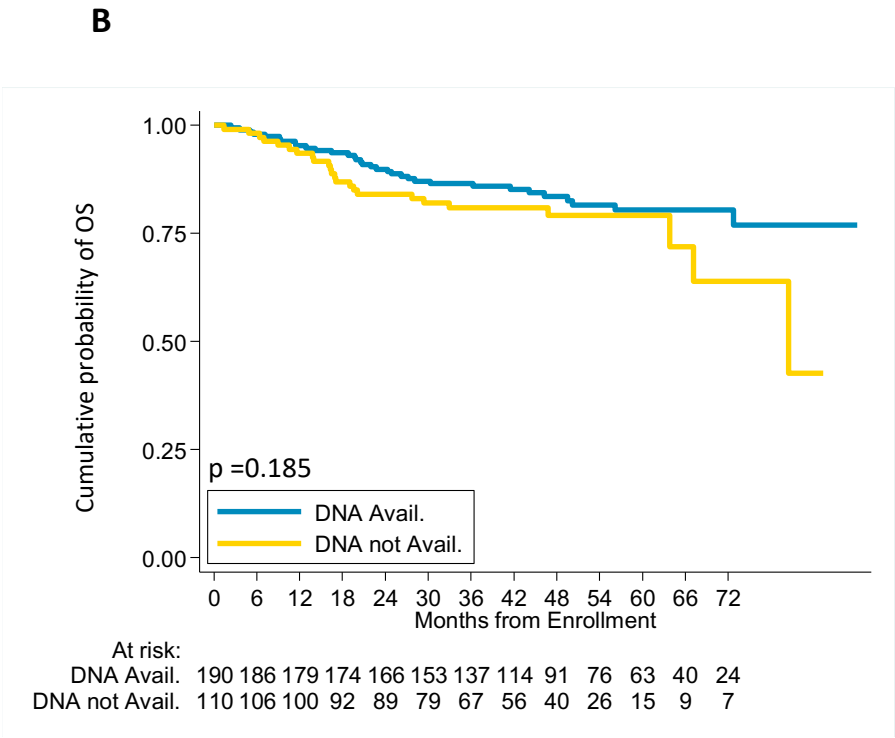
B
Cumulative probability of OS
1.00
0.75
0.50
0.25
0.00
p =0.185
DNA Avail.
DNA not Avail.
0 6 12 18 24 30 36 42 48 54 60 66 72
Months from Enrollment
At risk:
DNA Avail. 190 186 179 174 166 153 137 114 91 76 63 40 24
DNA not Avail. 110 106 100 92 89 79 67 56 40 26 15 9 7

Figure S1

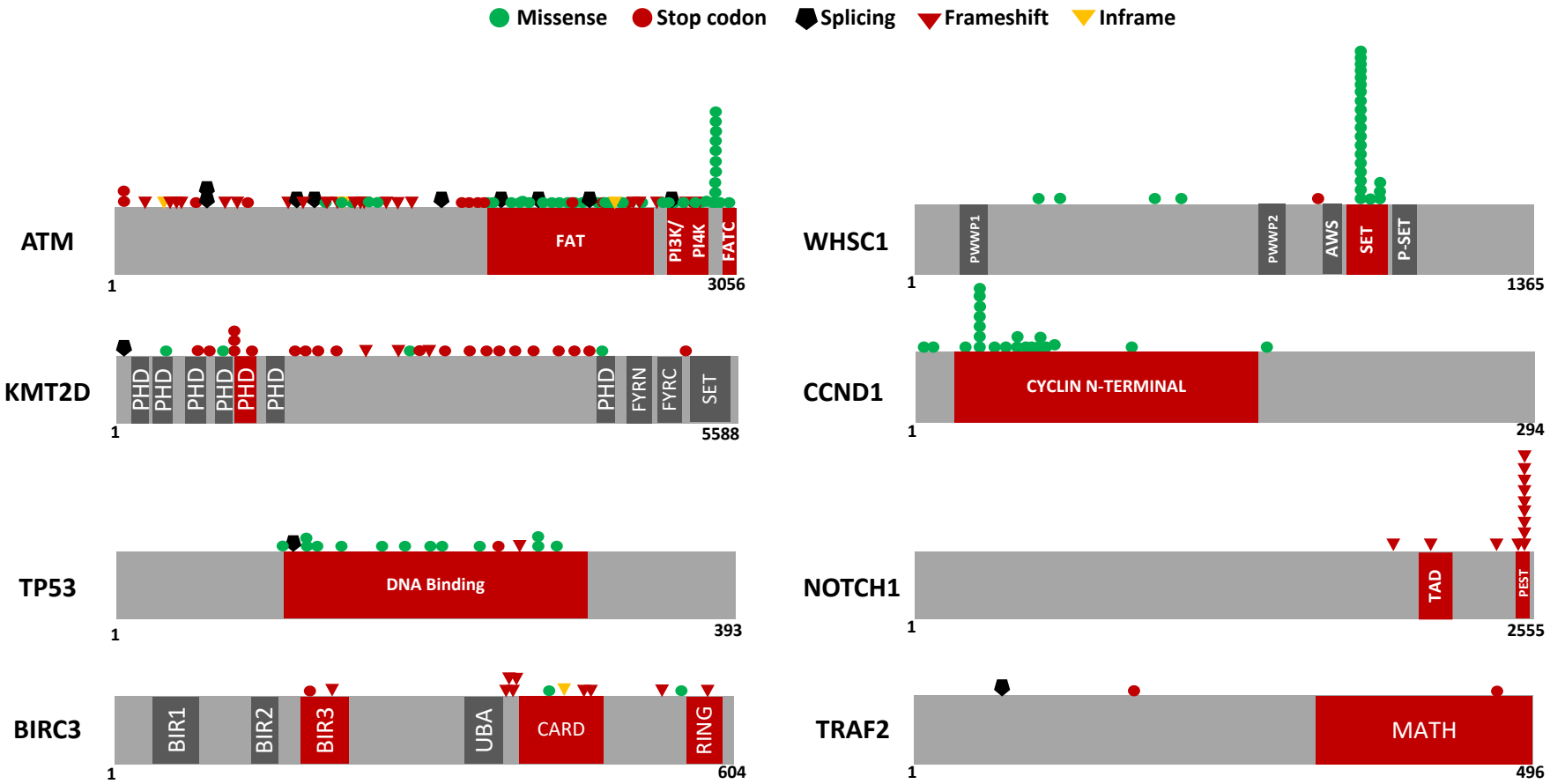
Missense
Stop codon
Splicing
Frameshift
Inframe
ATM
FAT
PI3K/
PI4K
FATC
1
3056
KMT2D
PHD
PHD
PHD
PHD
PHD
PHD
PHD
FYRN
FYRC
SET
1
5588
TP53
DNA Binding
1
393
BIRC3
BIR1
BIR2
BIR3
UBA
CARD
RING
1
604
WHSC1
PWWP1
PWWP2
AWS
SET
P-SET
1
1365
CCND1
CYCLIN N-TERMINAL
1
294
NOTCH1
TAD
PEST
1
2555
TRAF2
MATH
1
496

Figure S2

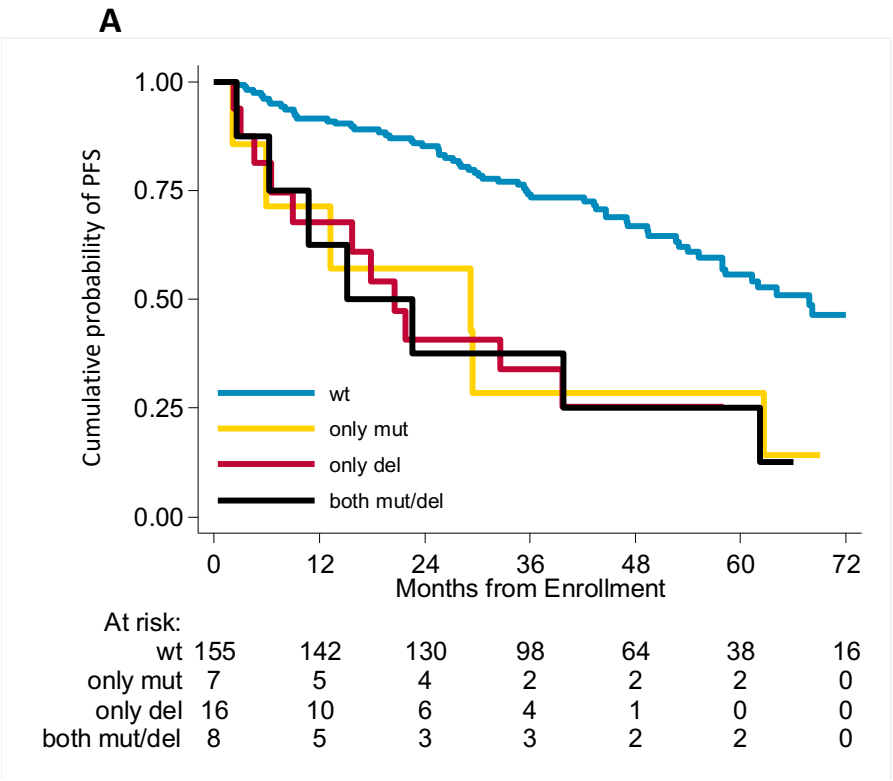
A
1.00
0.75
0.50
0.25
0.00
Cumulative probability of PFS
wt
only mut
only del
both mut/del
0
12
24
36
48
60
72
Months from Enrollment
At risk:
wt 155 142 130 98 64 38 16
only mut 7 5 4 2 2 2 0
only del 16 10 6 4 1 0 0
both mut/del 8 5 3 3 2 2 0

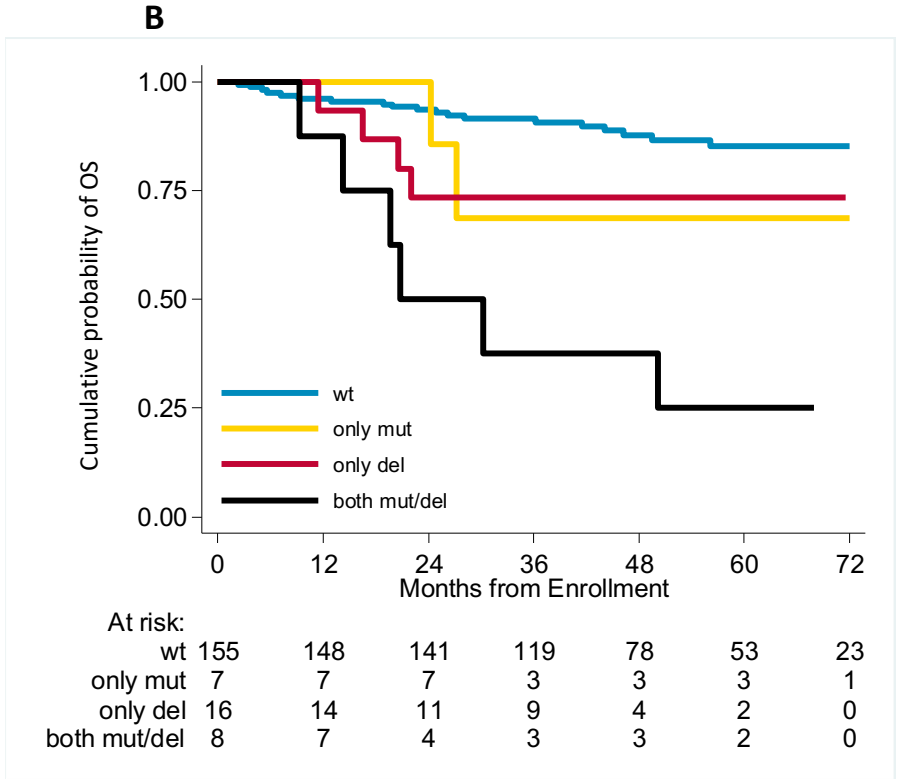
B
1.00
0.75
0.50
0.25
0.00
Cumulative probability of OS
wt
only mut
only del
both mut/del
0
12
24
36
48
60
72
Months from Enrollment
At risk:
wt 155 148 141 119 78 53 23
only mut 7 7 7 3 3 3 1
only del 16 14 11 9 4 2 0
both mut/del 8 7 4 3 3 2 0

Figure S3

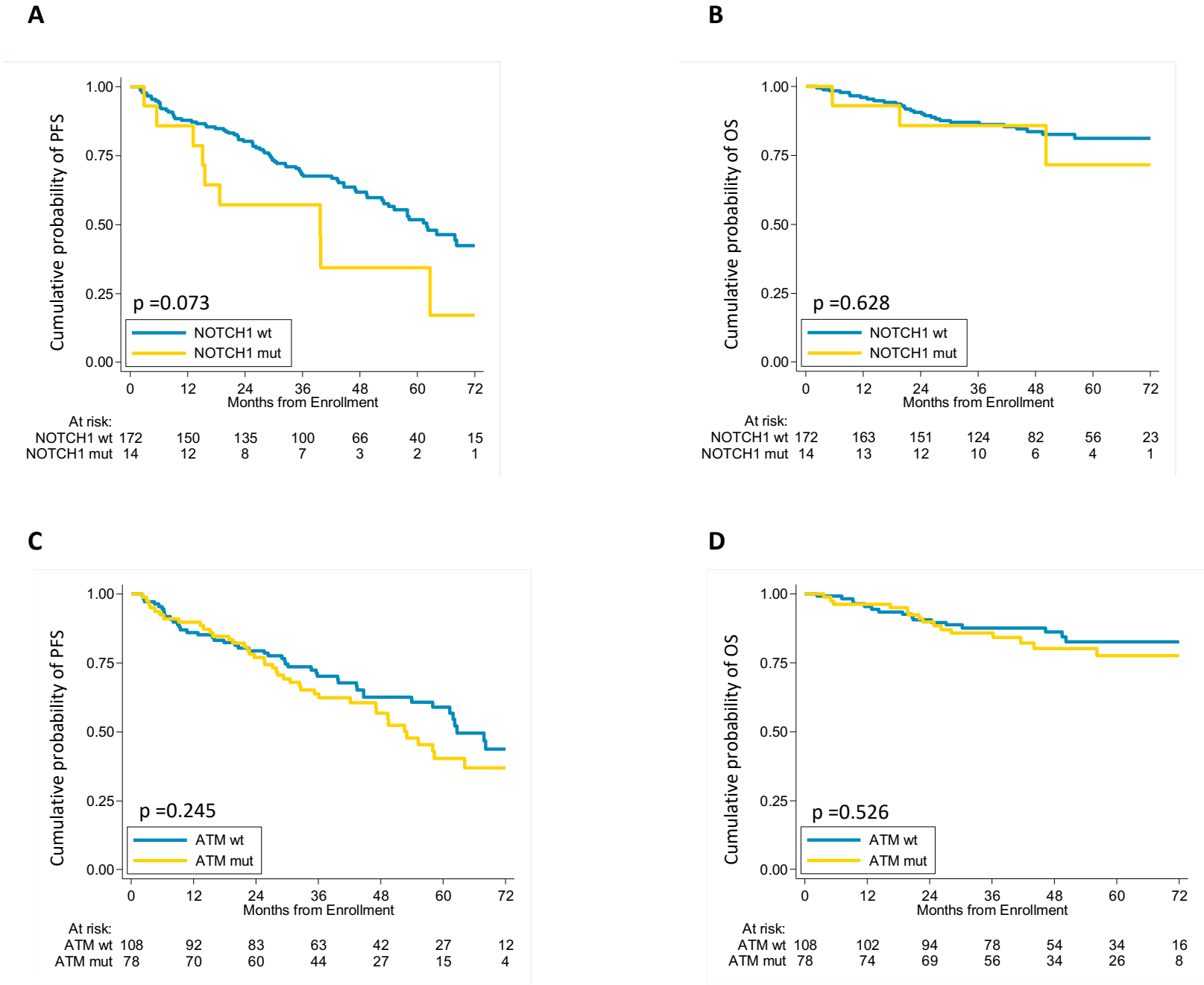
A
Cumulative probability of PFS
1.00
0.75
0.50
0.25
0.00
p =0.073
NOTCH1 wt
NOTCH1 mut
0 12 24 36 48 60 72
Months from Enrollment
At risk:
NOTCH1 wt 172 150 135 100 66 40 15
NOTCH1 mut 14 12 8 7 3 2 1
B
Cumulative probability of OS
1.00
0.75
0.50
0.25
0.00
p =0.628
NOTCH1 wt
NOTCH1 mut
0 12 24 36 48 60 72
Months from Enrollment
At risk:
NOTCH1 wt 172 163 151 124 82 56 23
NOTCH1 mut 14 13 12 10 6 4 1
C
Cumulative probability of PFS
1.00
0.75
0.50
0.25
0.00
p =0.245
ATM wt
ATM mut
0 12 24 36 48 60 72
Months from Enrollment
At risk:
ATM wt 108 92 83 63 42 27 12
ATM mut 78 70 60 44 27 15 4
D
Cumulative probability of OS
1.00
0.75
0.50
0.25
0.00
p =0.526
ATM wt
ATM mut
0 12 24 36 48 60 72
Months from Enrollment
At risk:
ATM wt 108 102 94 78 54 34 16
ATM mut 78 74 69 56 34 26 8

Figure S4

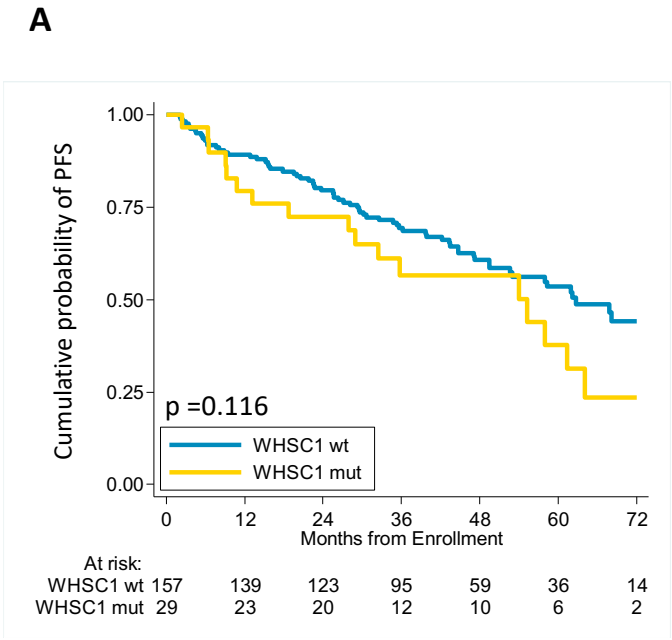
A
Cumulative probability of PFS
1.00
0.75
0.50
0.25
0.00
p =0.116
WHSC1 wt
WHSC1 mut
0
12
24
36
48
60
72
Months from Enrollment
At risk:
WHSC1 wt 157 139 123 95 59 36 14
WHSC1 mut 29 23 20 12 10 6 2

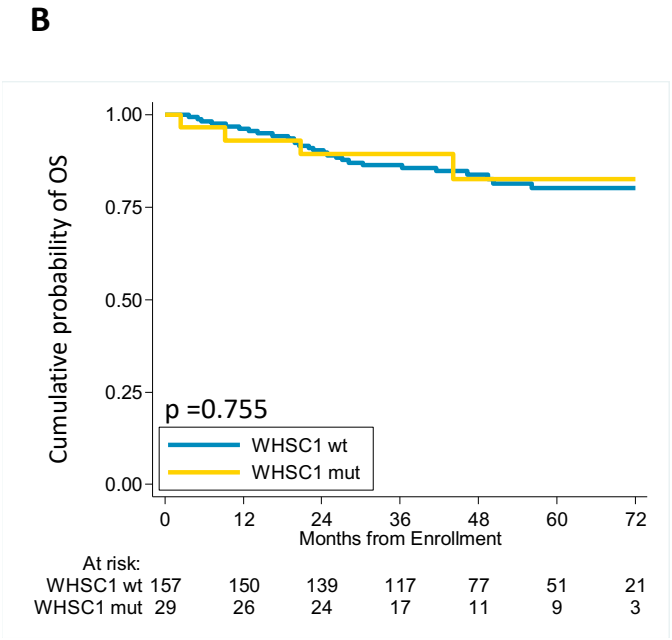
B
Cumulative probability of OS
1.00
0.75
0.50
0.25
0.00
p =0.755
WHSC1 wt
WHSC1 mut
0
12
24
36
48
60
72
Months from Enrollment
At risk:
WHSC1 wt 157 150 139 117 77 51 21
WHSC1 mut 29 26 24 17 11 9 3

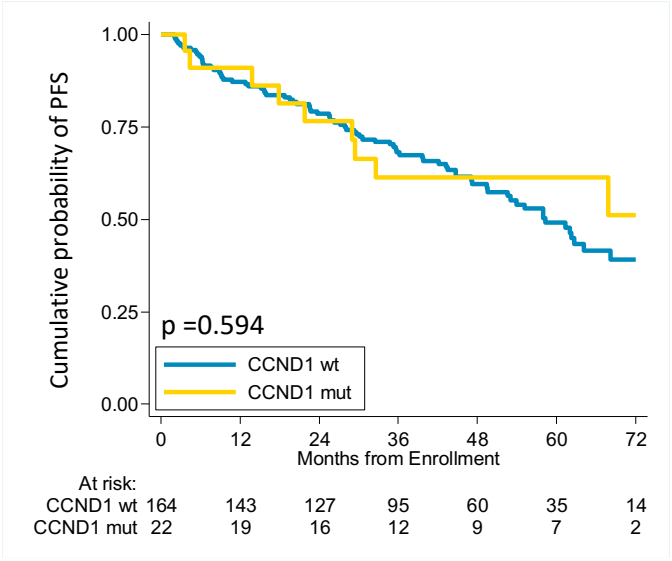
C
Cumulative probability of PFS
1.00
0.75
0.50
0.25
0.00
p =0.594
CCND1 wt
CCND1 mut
0
12
24
36
48
60
72
Months from Enrollment
At risk:
CCND1 wt 164 143 127 95 60 35 14
CCND1 mut 22 19 16 12 9 7 2

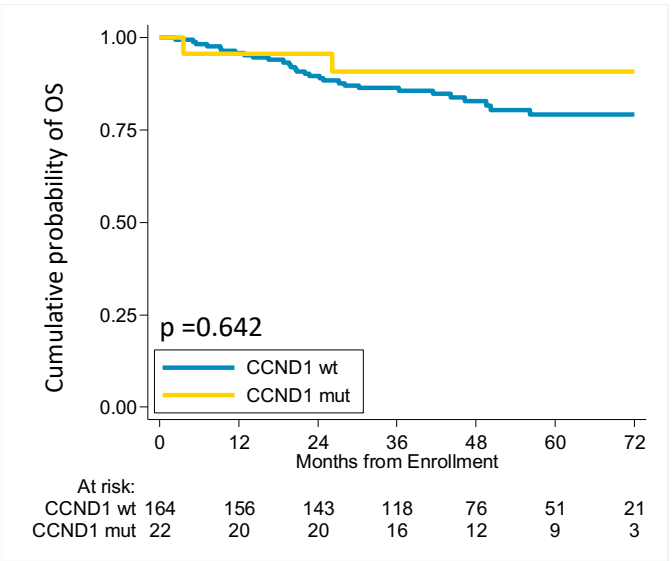
D
Cumulative probability of OS
1.00
0.75
0.50
0.25
0.00
p =0.642
CCND1 wt
CCND1 mut
0
12
24
36
48
60
72
Months from Enrollment
At risk:
CCND1 wt 164 156 143 118 76 51 21
CCND1 mut 22 20 20 16 12 9 3

Figure S5

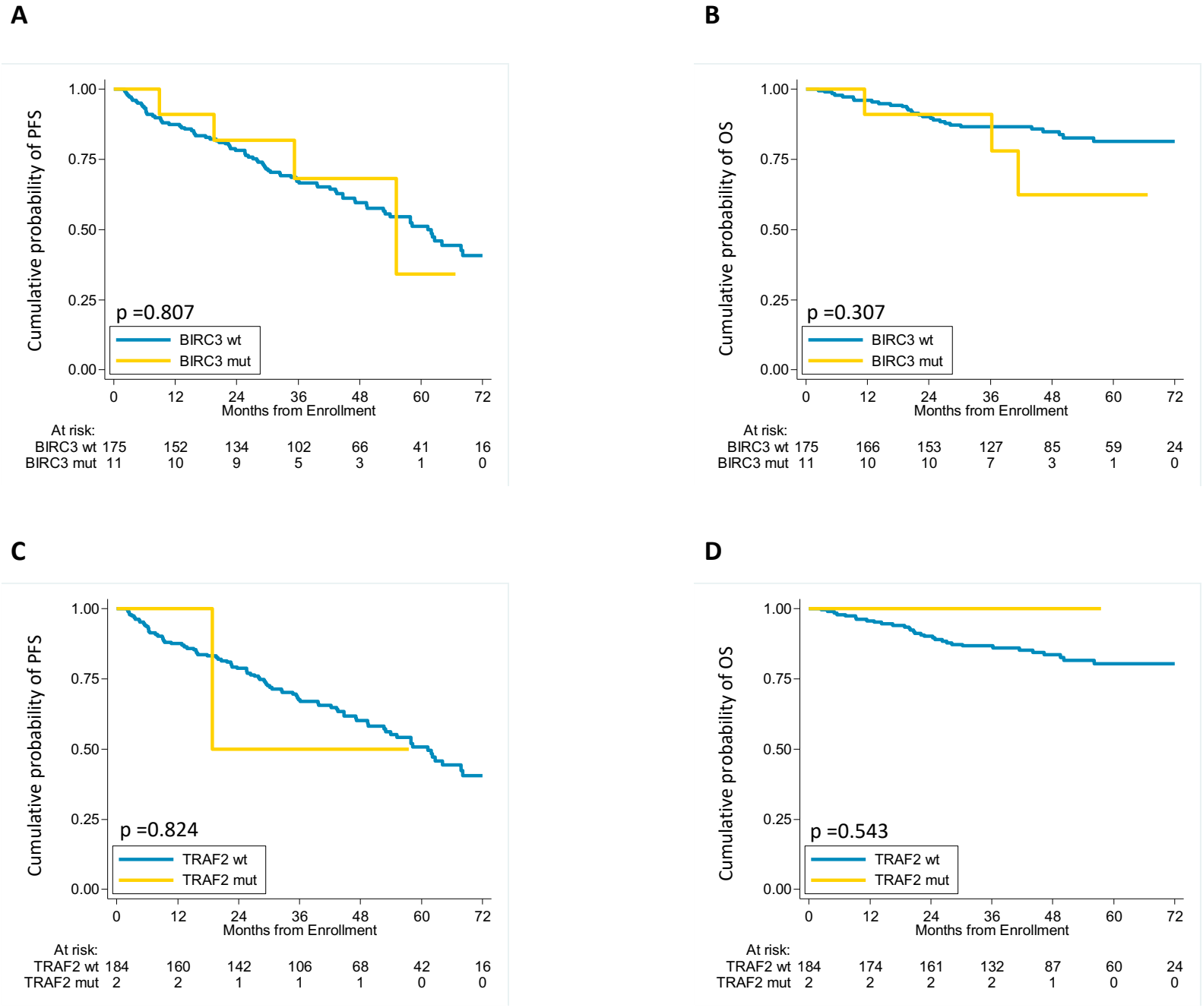
A
Cumulative probability of PFS
1.00
0.75
0.50
0.25
0.00
p =0.807
BIRC3 wt
BIRC3 mut
0 12 24 36 48 60 72
Months from Enrollment
At risk:
BIRC3 wt 175 152 134 102 66 41 16
BIRC3 mut 11 10 9 5 3 1 0
B
Cumulative probability of OS
1.00
0.75
0.50
0.25
0.00
p =0.307
BIRC3 wt
BIRC3 mut
0 12 24 36 48 60 72
Months from Enrollment
At risk:
BIRC3 wt 175 166 153 127 85 59 24
BIRC3 mut 11 10 10 7 3 1 0
C
Cumulative probability of PFS
1.00
0.75
0.50
0.25
0.00
p =0.824
TRAF2 wt
TRAF2 mut
0 12 24 36 48 60 72
Months from Enrollment
At risk:
TRAF2 wt 184 160 142 106 68 42 16
TRAF2 mut 2 2 1 1 1 0 0
D
Cumulative probability of OS
1.00
0.75
0.50
0.25
0.00
p =0.543
TRAF2 wt
TRAF2 mut
0 12 24 36 48 60 72
Months from Enrollment
At risk:
TRAF2 wt 184 174 161 132 87 60 24
TRAF2 mut 2 2 2 2 1 0 0

Figure S6

SUPPLEMENTARY TABLES EXCEL FILE ONLY

Table S1. Target region

Table S2. Somatic non-synonymous mutations discovered in the 186 cases of the molecular study

Table S3. Log-rank univariate analysis in terms of PFS and OS according to mutational status

Table S4. Clinical and biological baseline features of *KMT2D* and *TP53* disrupted patients

Table S5. MRD assessment after ASCT in *TP53* disrupted and in *KMT2D* mutated patients

Table S6. Multivariate analysis of *TP53* disruption and *KMT2D* mutations

SUPPLEMENTARY REFERENCES

1. Swerdlow SH, Campo E, Pileri SA, et al. The 2016 revision of the World Health Organization classification of lymphoid neoplasms. *Blood*. 2016;127(20):2375-2390.
2. Cortelazzo S, Martelli M, Ladetto M, et al. High Dose Sequential Chemotherapy with Rituximab and ASCT as First Line Therapy in Adult MCL Patients: Clinical and Molecular Response of the MCL0208 Trial, a FIL Study. *Haematologica.* 2015;100(s1): 3-4.
3. Beà S, Valdés-Mas R, Navarro A, et al. Landscape of somatic mutations and clonal evolution in mantle cell lymphoma. *Proc. Natl. Acad. Sci. U. S. A.* 2013;110(45):18250-18255.
4. Zhang J, Jima D, Moffitt AB, et al. The genomic landscape of mantle cell lymphoma is related to the epigenetically determined chromatin state of normal B cells. *Blood*. 2014;123(19):2988-2996.
5. Rahal R, Frick M, Romero R, et al. Pharmacological and genomic profiling identifies NF-κB-targeted treatment strategies for mantle cell lymphoma. *Nat. Med*. 2014;20(1):87-92.
6. Meissner B, Kridel R, Lim RS, et al. The E3 ubiquitin ligase UBR5 is recurrently mutated in mantle cell lymphoma. *Blood*. 2013;121(16):3161-3164.
7. Roccaro AM, Sacco A, Jimenez C, et al. C1013G/CXCR4 acts as a driver mutation of tumor progression and modulator of drug resistance in lymphoplasmacytic lymphoma. *Blood*. 2014;123(26):4120-4131.
8. Rinaldi A, Kwee I, Young KH, et al. Genome-wide high resolution DNA profiling of hairy cell leukaemia. *Br J Haematol*. 2013;162(4):566-569.
9. Kwee IW, Rinaldi A, de Campos CP, et al. Fast and Robust Segmentation of Copy Number Profiles Using Multi-Scale Edge Detection. *BioRxiv.* 2016. https://doi.org/10.1101/056705.

10. Voena C, Ladetto M, Astolfi M, et al. A novel nested-PCR strategy for the detection of rearranged immunoglobulin heavy-chain genes in B cell tumors. *Leukemia*. 1997;11(10):1793-1798.
11. Stamatopoulos K, Kosmas C, Belessi C, et al. Molecular analysis of bcl-1/IgH junctional sequences in mantle cell lymphoma: potential mechanism of the t(11;14) chromosomal translocation. *Br J Haematol*. 1999;105(1):190-197.
12. Pott C. Minimal residual disease detection in mantle cell lymphoma: technical aspects and clinical relevance. *Semin Hematol.* 2011;48(3):172-184.
13. Cheson BD, Pfistner B, Juweid ME, et al. Revised response criteria for malignant lymphoma. *J. Clin. Oncol.* 2007;25(5):579-586.